ASTRONOMY & ASTROPHYSICS
SUPPLEMENT SERIES

Astron. Astrophys. Suppl. Ser. **128,** 475-483 (1998)

B[e] stars

V. HD 50138 = MWC 158⋆

C. Jaschek[1] **and Y. Andrillat**[2]

[1] Observatoire de Strasbourg, URA 1280, CNRS 11, rue de l'Université, 67000 Strasbourg, France
[2] Laboratoire d'Astronomie Université de Montpellier 2, URA 1280 CNRS, Place Eugène Bataillon, 34095 Montpellier Cedex 5, France

Received June 5; accepted August 1, 1997

Abstract. On the basis of spectroscopic CCD material obtained at the Haute Provence Observatory, we provide line identifications and equivalent width measurements in the wavelength region 3738 – 10232 A of the spectrum of HD 50138 Over two hundred features are identified and a comparison of our results with those of other authors is provided. We also discuss the variability of the lines using equivalent widths and descriptions of the line spectrum. We attribute as a best compromise a spectral type of B 5 III. We conclude that the gaseous shell surrounding the star has a temperature of the order of 10 000 K and that its distance to the star is of the order of two stellar radii. We discuss the relation of this star to others previously analyzed and warn against hasty generalizations.

Key words: stars: emission line, B[e] — stars peculiar stars: HD 50138

1. Introduction

Balmer lines in emission were first detected in the line spectrum of HD 50138 by Merrill & Humason (1921). The first detailed description of the spectrum was made by Merrill (1931) who suggested the existence of two cycles of variability - a longer one of about five years and a shorter one of about thirthy days. He also found [O I] in weak emission. Later one a number of studies were devoted to the study of the blue spectrum, such as those by Struve & Swings (1940) and Swings & Struve (1943), Merrill (1952), Doazan (1960), Houziaux (1961) and Jaschek et al. (1980). The near infrared spectrum was studied by Houziaux (1961), Andrillat & Houziaux (1967), Jaschek et al. (1992) and the ultraviolet by Sitko et al. (1981) and by Hutsemekers (1985).

Allen & Swings (1976) classified the star into their group I, i.e. almost conventional Be stars with slightly extended atmospheres. The object is not associated with nebulosity and the interstellar and circumstellar extinction is small (< 0.10 m) From polarimetrc studies Vaidya et al. (1994, 1995) conclude that the star has a circumstellar disc. This is in line with its IRAS infrared excess (Hu Jingyao & Zhou Xu 1990).

Two recent outbursts of the star are documented: the first in 1978-9 (Hutsemekers) and the second in 1990-1 (Andrillat & Houziaux 1991; Bopp 1993).

Recently Pogodin (1997) has shown that a rapid day-to-day spectral variability exists too, through a study of the profiles of H_α, He I 5876 and the Na I lines.

The photometry of the star shows non-periodic variations of delta $V \sim 0.26$, delta $U - B \sim 0.10$, delta $B - V \sim 0.06$ delta $V - I \sim 0.06$ Kilkenny et al. 1985). Such ranges are confirmed by Halbedel (1991) who found no extra variations during the shell episode.

Jaschek et al. (1992) pointed out that the spectral types derived from the different spectral regions do not agree. These authors conclude that the object is intermediate between Be and B[e]. Such a classification disagrees with that of other authors who call the object a Herbig Be/Ae star. We shall come back to this point toward the end of the paper.

The aim of the present paper, as well of the others of this series, is to provide an identification list over an extended wavelength interval, together with a list of equivalent widths of the emission lines. This should lead to an improved understanding of B[e] stars and related objects.

2. Material

All the material, except one spectrum, was obtained on CCD receivers at the 193 cm telescope at the Haute

Send offprint requests to: Y. Andrillat

⋆ Table 2 is only available in electronic form at the CDS via anonymous ftp. 130.79.128.5 or via http://cdsweb.u-strasbg.fr/Abstract.html

Provence Observatory (OHP). The spectrograph used was CARELEC (Lemaitre et al. 1990). The observational data are collected in Table 1.

Table 1. Observational material for HD 50138

Region	Code	Date
3738 − 4189	a	04 - 04 - 93
3896 − 4335	b	25 - 10 - 91
4285 − 4724	c	23 - 10 - 91
4698 − 5138	d	25 - 10 - 91
6302 − 6724	e	23 - 02 - 92
6973 − 7402	f	24 - 10 - 91
7000 − 7444	g	06- 04 - 93
7570 − 7990	h	07 -01 - 90
7570 − 7994	i	29 -12 - 90
7583 − 8009	j	29 - 10 - 91
7586 − 8027	k	16 - 03 - 92
7613 − 8054	l	07 - 04 - 93
8305 − 8726	m	30 - 12 - 90
8358 − 8792	n	31 - 03 - 93
8360 − 8776	o	27 -12 - 90
8365 − 8785	p	21 - 02 - 92
8370 − 8790	q	15 - 11 - 89
9010 − 9425	r	27 - 12 - 90
9828 − 10232	s	18 - 04 - 92
9837 − 10241	t	22 - 02 - 92
9840 − 10232	u	14 - 11 - 89
3925 − 8060	v	07 - 03 - 96

For $\lambda < 6500$ A a grating with 1200 lines/mm, blazed at 4000 A was used, providing a dispersion of 33 A/mm in the first order. For $\lambda > 6500$ A a 1200 lines/mm grating was used, with a blaze at 7500 A which provides in the first order a dispersion of 33 A/mm; filt er OG 590 was used to cut out the second order.

In 1989 the receiver was an RCA CCD with 323×512 pixels (30 square microns), providing a resolving power of 1.7 A/mm. From 1990 to 1993 the receiver was a Thomson CCD with 512×384 pixels, (23 square microns), providing a resolving power of 1 A. After 1993 the receiver used was a TK 512 CCD, with 512×512 pixels (27 square microns). The resolving power was about 1.2 A.

For the wavelength calibration we used Ne, Ar and He lamps. Flat field corrections were made with a Tungsten lamp mounted in the spectrograph. The slit width used was 300 microns, corresponding to $2''$ on the sky.

The data were reduced with the software package IHAP, developed at ESO and installed at the OHP.

The only spectrum not taken at the OHP was obtained by Dr. D. Ballereau at the Argentinian Observatory of CASLEO, with the 215 cm telescope, and generously loaned to the authors. The spectrograph is a REOSC type Cassegrain, the receiver a CCD TEK, 1024×1024 pixel, and the resolution 0.45 A/mm at 3700 and 0.72 at 6000 A. The reduction programs were made by M.Chauville from the Paris Observatory.

As remarked above, the resolving power is of about one Angstroem, which is not very well suited for radial velocity studies.The smallest equivalent width which can be measured is of the order of 0.15 A. Since we are working with material obtained under the same conditions as those for HD 51585 (Jaschek et al. 1996 = Paper I) we adopt the errors given in that paper which are of the order of $\pm 10\%$. Furth ermore, the resolution prevents us also from resolving structures in the line profiles (double lines for instance) whose separation is less than 75 km/s in the blue and 40 km/s in the red.

3. Line identifications

These were made in the traditional way, paying attention to both wavelengths and line intensities within the multiplets.

The identifications were made with the help of the table of Moore (1959); for Fe II we also used Johansson's (1978) complation and for [NiII] Nussbaumer & Storey (1982). In addition we have used the Meinel et al. (1969) catalogue, for lines which we could not identify (see notes to Table 2).

On our spectra are present 217 features, of which 40% are pure absorption lines whereas the majority is constituted by emission lines. We were unable to identify 7% of the lines, which is about normal in identification work. Furthermore 33% of all lines are produced by Fe II and [Fe II] The complete list of identifications is given in Table 2. Parts of the spectrum are reproduced in Fig. 1. The Paschen region, at different epochs is illustrated in Fig. 3 and the O I region in Fig. 4.

From Table 2 and Figs. 1 and 3 it can be seen that up to 4200 A the spectrum is mostly formed by absorption lines, whereas beyond 4200 the emission lines start to predominate. After 6300 the absorption lines do constitute an exception. We shall thus fix, somewhat arbitrarily, $\lambda = 5500$ as the point where the shell starts to predominate over the underlying spectrum.

In what follows, we will describe first the identifications, element by element and then the structures present in the lines of different elements Since, as can be seen from Table 1, the material was taken at different dates, the discussion of the structures is directly linked with that of spectrum variability.

4. The behavior of the elements

Hydrogen. The Balmer series is present in absorption from H12 to H 3. Structures are present from H5 to H 3. The Paschen lines are observed from P 25 to P 12 and P10, 9 and 7. All the lines are in emission and show structure. The underlying absorption lines are only visible sometimes. The spectral type, as derived from the equivalent

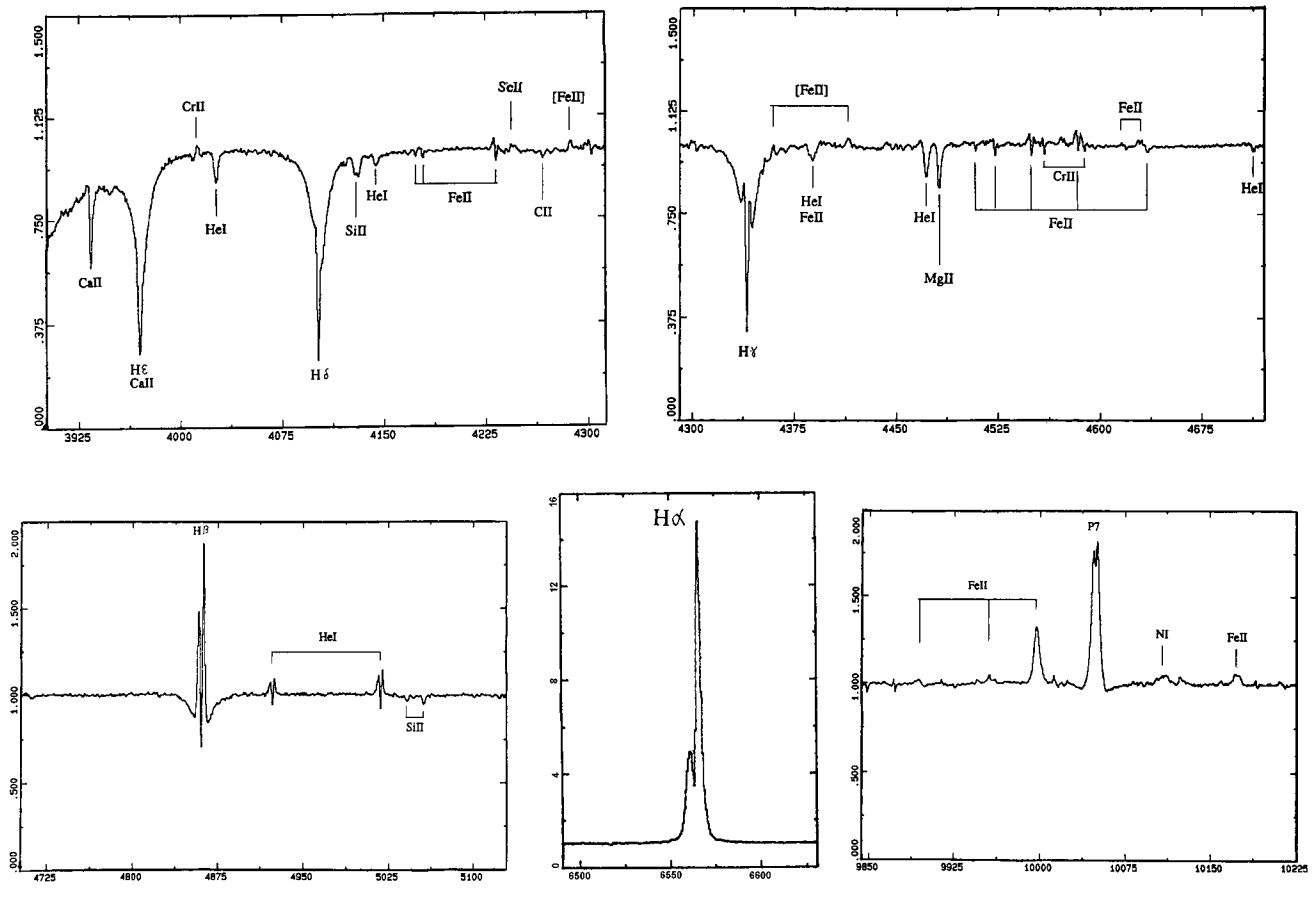

Fig. 1. Reproduction of CCD spectra of HD 50138. Abscissae: wavelengths in A. Ordinates: intensities. The continuum is set to unity. Important lines are identified. The spectra correspond to $\lambda\lambda$ 3925−4300 (from 25.10.91), $\lambda\lambda$ 4300−4575 (from 23.10.91), $\lambda\lambda$ 4725−5100 (from 25.10.91), $\lambda\lambda$ 6500−6600 (from 23.2.92) and $\lambda\lambda$ 9850−10225 (from 14.11.89)

width of the H6 line, corres-ponds to B 5. The Paschen line emissions are usually found only in earlier types.

Helium. Of the neutral helium series are present the lines of the $^1P^0$, ^3S, ^3D and ^1D series. The profiles are generally in clean absorption, except for three lines, which show structures. The line 3889 from the $3P^0$ series is probably also present, as can be judged from the wavelength of the blend He I+ H8.

The helium lines correspond in strength to B7-8 III. It is therefore a surprise to see the He II line 10123, seen only in much hotter objects. (O to B0). No other He II line is seen, and the line was observed only in 1989.

Carbon. Ionized carbon is represented by a weak absorption line 4267 from M.6, whose strength is compatible with B 5 III, and by lines from M.14 and 37.

Nitrogen. Neutral nitrogen is well represented by emission lines from M.1, 7, 8 and 18.

Ionized nitrogen is represented by one line from M.46 (λ 6340).

Oxygen. Neutral oxygen is represented by lines from M.1, 3, 4, 8, 10 and 12. M.1, 3, 10 and 12 are seen in absorption, whereas 4 and 8 are seen in emission. Both 7774 (1) as well as 8446 (4) are strongly variable. 8446 appears in emission (as said before) and is stronger than expected, a fact which is due to fluorescence from Lyman beta.

Forbidden neutral oxygen is represented by two rather strong lines from M.1 and 3.

Magnesium. Neutral magnesium is represented by M.1(λ 4571), 8 ($\lambda\lambda$ 7878+7898) and 9(λ 5528) in absorption but with an accompanying emission and by M.23 and 27 in emission.

Ionized magnesium is represented by lines from M.1, 4, 17 and 20. M.1 is in emission, whereas the others are in absorption. Its intensity corresponds to about B5 Ia. The presence of Mg I is therefore unexpected, since it appears in A type stars.

Aluminum. Ionized aluminum is represented by one emission line from M.40. The presence of this element is doubtful.

Silicon. Ionized silicon is represented by absorption lines from M.1, 2, 3 and 5. Their strengths are compatible with a spectral type B 5 III.

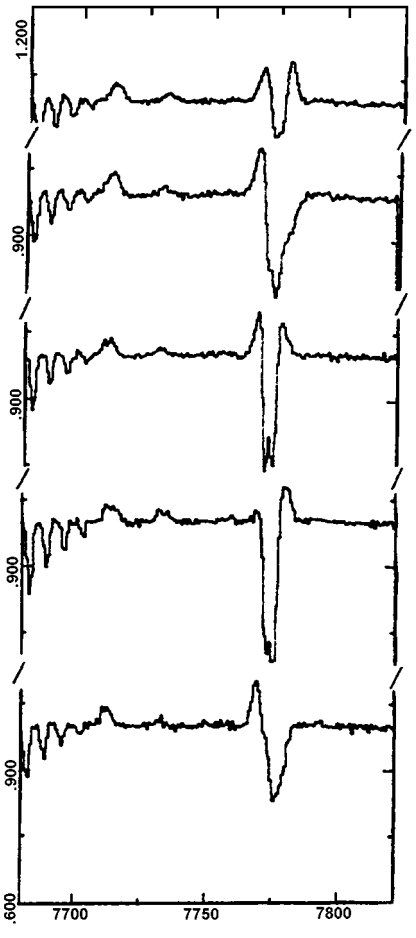

Fig. 2. Variations in the profil of O I 7774. From top to bottom, the spectra were taken on 07.01.90−29.12.90−29.10.91 −16.3.92 and 07.04.93. Two iron lines are also visible: l 7712 Fe II and λ 7732 Fe II+[Fe II]

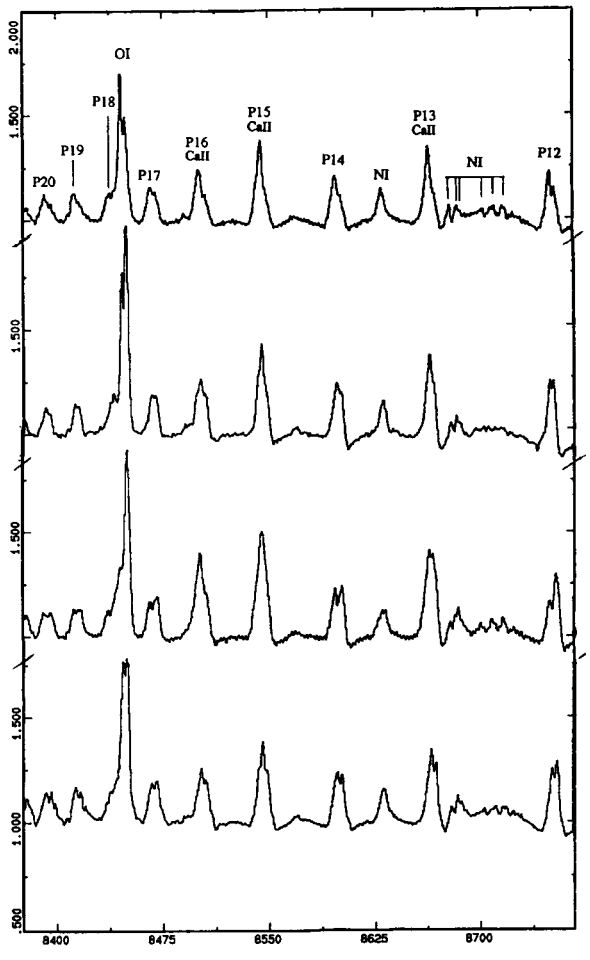

Fig. 3. Variations in the region P12 to P20. From top to bottom, the spectra were taken on 15.11.89−27.12.90−21.2.92 and 31.03.93

Sulphur. Forbidden ionized sulphur is represented by λ 4068 which exhibits an emission- absorption structure and 4076 which is in absorption, both from M.1.

Calcium. Ionized calcium is represented by lines from M.1 and 2. Whereas the EW of 3933 (M.1) corresponds to about A0, lines of M.2 are not always present and appear in emission. If the Paschen lines are substracted, the lines of M.2 have intensities which correspond to the laboratory intensity. In early type stars such ratios, which indicate an optically thin emitting medium, are unusual.

Scandium. Ionized scandium is represented by the emission line λ 4246 from M.7.

Titanium. One line from neutral forbidden titanium (λ 4522) is present. Ionized titanium is represented by emission lines from M.19 and [Ti II] by lines from M.5 and 22.

Chromium. Ionized chromium is represented by three lines from M.44 and one line from M.30 (in absorption) and M.24, 43 and 183 (in emission). The lines of M.44 show absorption/emission structure.

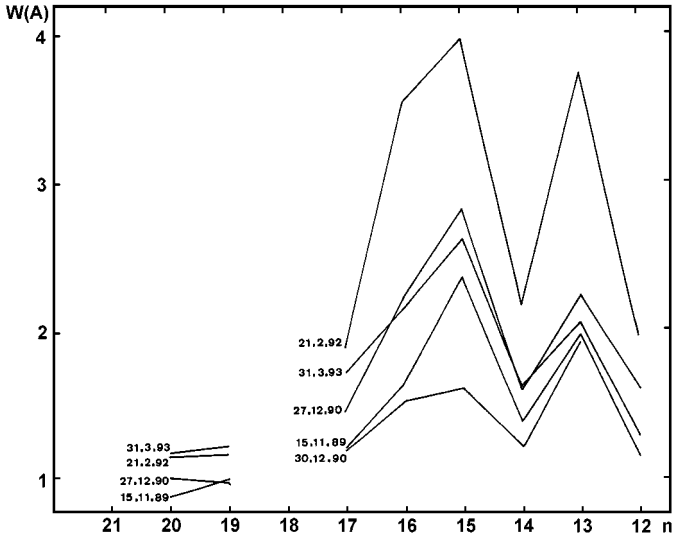

Fig. 4. The equivalent width of the Paschen lines at different dates. Abscissae: principal quantum number n. Ordinates: equivalent widths in A

[Cr II] is represented by two features from M.10 and 14.

Vanadium. Three lines from M.3 and 4 of forbidden ionized vanadium are present.

Iron. Ionized iron is well represented by absorption lines from M.26, 27, 28, 36, 37, 38, 42, 48, 49, 73, 74 and 186 plus emission lines from M.41. Many lines from M.27, 28, 37, 38, 42 and 49 show structures. Probably even more would show up at higher resolution. [Fe II] is represented by numerous emission lines from M.1, 4, 6, 7, 14, 16, 18, 19, 20, 33, 41 and 44.

Zirconium. Ionized forbidden zirconium is represented by some lines from M.4 and 12.

A summary of the elements present is given in Table 3, which lists also the elements identified by other authors, namely Houziaux (1961), Doazan (1965) and Hutsemekers (1985). In general the coincidence is as well as can be expected, because the four identification works were not based upon the same wavelength regions. The only cases in which the non detection indicates a possible variability are; C II, O II, [S II] and V II.

5. Structures present in the lines of different elements

Despite the fact that our material was taken at several different dates and is not large enough to permit a follow up of the variations, we provide in what follows a detailed description of what is seen on our spectra. The reasons are twofold: the history of the star is a very complex one and even isolated bits of information are valuable for the general picture and second, because we present for the first time a collection of equivalent widths. Much of the previous material was based upon photographic plates, which are difficult to calibrate accurately.

Hydrogen. Practically all Balmer lines show structures. H 7 (from 04.04.93) appears as a sligthly asymmetri c line, as if an unresolved emission component were present on the red border. H 6 (from 02.10.91) has an asymmetric profile, with unresolved emission components on both the violet and the red of the absorption line center. The wing is clearly steeper on the red border. In 1996 a sharp line core is visible, with a small red emission component. H 5 (from 23.10.91) shows a violet and a red emission, separated respectively 166 and 110 km/s from the absorption line center, with $V > R$. This corresponds well with what is also observed in H 6, taken both in October 1991. In 1996 one sees very well the central sharp absorption superimposed upon the broad absorption line. The central absorption is flanked by two emission borders, with $R \gg V$.

H 4 (25.10.91) shows a rather broad absorption line extending over 50 A (3000 km/s) upon which two intense emission components are seen, separated by a sharp central autoreversal. The violet and red peaks are separated by 150 and 100 km/s respectively from the autoabsorption line center. One sees $V < R$ with equivalent widths of both emission components, measured from the continuum level, of 0.96 and 1.59 respectively. The emission line structure seem to be displaced toward the violet of the absorption line center. Since the absorption line is ill defined, the displacement can only be estimated to lie around 100 km/s In 1997 the profile is rather similar, with $R \gg V$. Within the uncertainties of the absorption line, the

Table 3. Elements present in HD 50138

	PP	H	D	Hu
H	p	p	p	
He I	p	p	p	
He II	(p)			
C I				p
C II	p			p
C IV				p
N I	p			p
II	p			
O I	p	p		p
[OI]	p	p		p
O II		p		
Na I	p			p
Mg I	p	p	p	p
II	p	p	p	p
Al II	p			p
Al III				p
Si II	p	p	p	p
Si III				p
Si IV				p
S II				p
[SII]	p			p
P II				p
P III				p
Ca II	p	p	p	
Sc II	p		p	
[TiI]	p?			
[TiII]	p	p	p	
Ti III				p
V II	p			
Cr II	p	p	p	p
Mn II				p
Fe I		p?		
Fe II	p	p	p	p
III				p
Ni II		p?	p	p
Zr II	p	p?		

PP = present paper. For the wavelength region covered see Table 1.
H = Houziaux (1961) ll 3642 − 8544.
D = Doazan (1965) ll 3814 − 6678.
Hu = Hutsemekers (1985). ll 1253 − 1937 2011 − 3132. The only emission lines seen correspond to Mg II and Fe II.

emission structure seems more centered upon the absorption line profile than formerly.

H 3 (from 25.10.91) is seen only as an emission feature, with two peaks; the autoabsorption does not reach the continuum level. $V \ll R$ and the separation between the two peaks is of 220 km/s. The equivalent width of the e mission is of 61 A. The total width of the line seems to be of the order of 3700 km/s. The total width of the line is even larger in 1996, reaching 6000 km/s.

Paschen series.

The phenomena in the Paschen series (see Fig. 3) are best summarized in tabular form. Table 4 groups the principal features. We add some comments which do not fit in the table. In 1990 the profile of the underlying absorption line is much stronger on the red side, on the 27.12. Three days later the violet wing has almost disappeared, so that one has the impression of an inversed P Cyg profile, and this is also true for the spectra of 1992 and 1993.

P 9 in 1990 has a double peak, with $V = R$, and a separation of 30 km/s. It must be mentioned that the existence of the double peak is somewhat doubtful, in view of the numerous components of atmospheric absorption.

P 7 in 1989 has a double structure, with $V < R$ and peak separation of 95 km/s. In 1992, $V \ll R$, with 145 km/s of peak separation.

As can be seen from Table 4 and Fig. 4, there exists no clear progression in the peak separations with the Paschen number, even within the same spectrum. We have also listed the equivalent widths (see Table 5). It should be stated that these values are somewhat uncertain in the higher numbers, because of the confluence of the Balmer lines. In the lower numbers we see the underlying absorption and we have then the difficulty in defining what to measure. Whenever possible we have made both the measures from the interpolated continuum and from the underlying absorption line. Usually the measures differ considerably, up to almost a factor of two, the measures from the absorption profile being of course the larger ones.

As already said, the present material is much too limited in time coverage as to permit to draw useful conclusions, except the obvious one that the structures vary strongly over very short time intervals and that the variations can be up to 100% in equivalent width. We stress the fact that these are the first systematic measures of equivalent widths for this object.

Helium. Structures are present in some lines. λ 4471(^{3}D) observed on October 21, 1991, has the violet wing in emission, at a distance of 320 km/s from the center of the absorption line. In 1996 the broad underlying photospheric line is well visible and the violet emission line is found at about 280 km/s.

In λ 4921, of the ^{1}D series, (25.10.1991) the absorption line is flanked by two emission peaks, which are symmetrically placed around the absorption line, at a distance of 100 km/s, with $V < R$. In 1996 the appearance is about the same, but the violet emission is much broader than the violet one and structure is perceptible in both emission components. Also the forbidden line at 4920 is visible.

The λ 5015 line of the ^{1}P^0 serie (25.10.1991), is flanked by two emissions separated 190 km/s, $V < R$. In 1996,we find a broad emission feature divided by an absorption peak, which leaves a narrower violet component and a broader red component, with $V > R$.

The λ 5875 line has its violet wing in emission in 1996. We have examined also the other He I lines present at this date and we find about normal absorption profiles, although in a number of lines one suspects a broad violet emission feature.

Oxygen. The variations in the profiles of O I λ 7774 and 8446 are also very large. The variations are illustrated in Figs. 2 and 3.

The λ 7774 line is an absorption line, with adjacent emission structures. For 7774 we find on 7.1.90 a double emission structure with a central absorption, the emission peaks being about equal and located at -285 and $+165$ km/s from the absorption line center, WE/WA = 1.65. On the 29.12.90 the red emission has disappeared, whereas the violet is found at -245 km/s, WE/WA = 0.22. On 29.10.91 we have two symmetric emissions, with $V = R$, displaced -155 and $+25$ km/s from the average of the two absorption lines, which are interrupted by a central emission peak., with WE/WA = 0.44. On 16.3.92 the structure is similar, except that now $V \ll R$, with separations of -210 and $+245$ km/s, with WE/WA = 0.19. On 7.4.93, the profile is similar to that of the 29.12.90, with a similar displacement of -245 km/s, with WE/WA = 0.42. In the preceding WE/WA stands for the ratio of the equivalent widths of the emissions over the absorption, counted from the interpolated continuum. As can be seen, in general the absorption predominates, except in the first spectrum. In 1996 (Jan. 9) the line presents a rather complicated structure. We have first the absorption line at λ 7776, accompanied by two broad emission features, with $V > R$. The violet one is about 380 km/s broad and the red, 250 km/s. On the violet wing one sees a further absorption, displaced 150 km/s from the main absorption line. The variations of the λ 8446 line are more difficult to follow, because of the blend with P 18. The line is however always in strong emission. On 15.11.89, we have $V \gg R$, peak separation 100 km/s, $W = 4.0$ A. On 27.12.90, we find $V \ll R$, peak separation 115 km/s, $W = 4.5$ A. On 30.12.90 (three days later) we find no double structure, $W = 4.08$ A. On 21.2.92 we find $V \ll R$, peak separation 170 km/s, $W = 5.1$ A. On 31.3.93 we find two peaks of similar height, with separation of 95 km/s and $W = 5.2$ A. In all cases we have discounted the extrapolated equivalent width of P 18. It should be added that the structure of O I does not run parallel to that of the Paschen lines- for instance on 27.12.90 we find $V \ll R$ for O I and $V > R$

Table 4. Description of the Paschen series

Paschen	15.11.	27.12.	30.12.	21.2.	31.3.
	1989	1990	1990	1992	1993
P 21	–		s	200	130
P 20	s	100	–	170	130
P 19	70	85	s	143*	130*
P 18&	$V > R$	$V < R$	s	s	$V < R$
P 17	150*	85*	60*	55*	20*
	$V >= R$	$V = R$	$V = R$	$V \Leftarrow R$	$V \Leftarrow R$
P 16&&	170	115	s	s,nm	95
	A	A	A		
P 15&&	115	115	s	s	95
	A	A	A	A	A
P 14	140	110	60	165	95
	A	$V > R, A$	$V = R^*, A$	$V = R^*, A$	$V = R^*, A$
P 13&&	120	85	s	85*	125*
	A	A	A	$V = R, A$	$V > R, A$
P 12	110*	85*	125*	125*	
	$V > R, A$	$V = R, A$		$V < R, A$	$V < R, A$

The table provides for each Paschen line the separation between the components, in km/s, s = single. The second line provides the relation between the violet(V) and red(R) components. An asterisk means that the two peaks are well visible. A = stands for an underlying absorption line. & in the first column stands for a blend with O I, && for a blend with Ca II.

Table 5. Equivalent widths of the Paschen lines

Paschen	15.11.	27.12.	30.12.	21.2.	31.3.	Notes
	1989	1990	1990	1992	1993	
P 25	-	-	0.10	-	-	
P 23	-	-	0.25	-	-	
P 22	-	-	0.09	-	-	
P 21	-	0.92	nm	1.14	1.01	
P 20	0.89	1.02	0.26	1.15	1.19	
	1.09					
P 19	1.02	0.99	0.36	1.18	1.23	
	1.17					
P 18	nm	nm	0.62	nm	nm	Blend O I
P 17	1.21	1.45	1.20	1.88	1.73	
	1.24					
P 16	1.64	2.23	1.54	3.54	2.15	Blend Ca II
	1.98	2.30		4.22	2.43	
P 15	2.36	2.82	1.61	3.96	2.61	Blend Ca II
	2.76	3.25		4.57	3.22	
P 14	1.39	1.60	1.21	2.17	1.61	
	1.94	2.36		2.46	2.31	
P 13	1.97	2.24	1.94	3.74	2.05	Blend Ca II
	2.61	3.38		4.22	3.21	
P 12	1.16	1.60	-	1.96	1.28	
	2.21	3.03		3.04	2.74	

The table provides in the first line the equivalent width measured from the interpolated continuous spectrum and in the second line the equivalent width measured from the lower points of the underlying absorption line. For the spectrum from 30.12.90, see text. nm = non measured.

for the Paschen lines. On other dates they are roughly parallel.

The profiles of the other O I lines present on the 1996 spectrum do not show structures.

Calcium. On the spectrum from 07.03.96 one observes λ 3933 as a sharp absorption lines, accompanied by an emission structure, broader on the V than on the red, and with $V > R$. The λ 3973 line shows a sharp absorption core, accompanied by two sharp satellite absorption lines, located respectively at +850 and +1200 km/s. We have attributed these two lines to Ca II, because of the similarity of the line profiles and because we were unable to find a satisfactory identification for the two lines The less displaced line is more intense than the other.

Heavier elements. Some lines of ionized iron (4232 and 4303 from M.27; 4549 and 4583 from M.38 and 4629 from M.37) and of ionized chromium (4558 and 4588 from M.44) do show structures. The structures appear as emission wings accompanying the absorption line, with $V > R$, the red emission being sometimes very weak or invisible. The emission separation is of the order of 200 km/s. All lines in which this structure is visible are the strongest of their respective multiplets, so that it cannot be discarded that with better resolution, all ionized metal lines could show such a structure.

The phenomenon of the variable emission structures has been described in the past by several observers, first by Doazan (1960) and then, among others, by Hubert-Delplace & Hubert (1979).

We have also looked into the variations of equivalent width of the few lines which happen to be present on two spectra taken on different dates. We find variations of up to a factor two in the equivalent widths, but the material is too scanty to permit to draw more conclusions. We had already found variations of such an amount in the Paschen lines of this star and moreover variations of such an amount are also present in other B[e] objects.

6. The spectral type of HD 50138

In what precedes, we have seen that the absorption lines do not permit to attribute a unique spectral type to the star. The equivalent widths of H delta gave B5; the He I lines, B7-8 III; Ca II (3933), A0; Si II, B 5 III; Mg II (4481) B 5 Ia and finally CII (4267) gives B 5 III. Furthermore we remark that the emission lines present (Fe II, [FeII], N I) are usually found only in stars earlier than B 5. We recall that Houziaux (1961) classed the star as B 5 IV and Doazan B 5 V, the former from low dispersion spectra and the latter from high dispersion spectra. We adopt finally B 5 III from Jaschek et al. (1992) as the best spectral type for the blue spectral region.

Outside the present spectral range, the star was classified in the near ultraviolet as B9 pec by Heck et al. (1984); Hutsemekers calls it B 8.

We recall that we found a similar inconsistency of the spectral type from the blue region and the ultraviolet in the case of HD 45677, a star which shares many characteristics with the present one.

A luminosity class III is also compatible with the astrometric data. The distance of the star would be 450 pc. The proper motion (0″014 /year) gives then 30 km/s, the galactic latitude (−3.1) a heigth of 27 pc above the galactic plane and even the small interstellar extinction (<= 0.10) would be compatible with the relatively small distance.

7. The temperature of the shell

We shall now try to obtain an idea about the temperature of the shell using the presence of the elements observed in emission, as we have done in other papers of this series. Judging from the the ionization stage of the elements present in emission, we can say that the spectum corresponds to a late B or early A type object, a fact which would place the temperature of the shell at about 10 000 K. Assuming the photospheric temperature to be 15 000 K, and a black- body model for the two entities, one can calculate the radius of a surface which would dominate at wavelengths beyond 5 500 A, which is what one observes. It results a radius of 1.6 times the radius of a 15 000 degree star, which would correspond to the distance of the shell. This is rather close to the surface of the star, but is in line with the radius which can be deduced from the H alpha profile (Jaschek & Jaschek 1993) and which gives 2.7 stellar radii.

8. Is HD 50138 a typical B[e] star?

We would like to conclude with a comment on the group into which HD 50138 can be classified. It has usually been put either in the group of B[e] stars (Bopp 1993) or in the group of Herbig Be-Ae stars (Morrison & Beaver 1995). From the definitions of the groups (see Jaschek & Jaschek 1987), it is difficult to conclude that the object belongs clearly to either one of them. It has certainly many forbidden lines in emission, as required by B[e] stars, but contrary to other stars of the group, one perceives the photospheric spectrum of the underlying star. With regard to the membership in the group of Herbig Be-Ae stars, one of the original criteria was the existence of an associated nebulosity, which in HD 45677 is abs ent. It is thus not a Herbig Be-Ae star. Also Thé et al. (1994) do not include it in their catalogue of Herbig Ae/Be stars.

The fact that three stars analysed up to now in this series (MWC 51585, MWC 349A and MWC 645) do not show any absorption lines, whereas HD 50138 (as well as HD 45677) do show absorption lines, provides a clear indication of (at least) two subgroups of B[e] stars. Until many more stars of the group are analysed, it seems premature to call HD 50138 (or MWC 645) a typical B[e]

star. Caution is thus recommended a Nnd one should not apply whatever is known on this particular star to other B[e] stars. The same applies of course to models.

Acknowledgements. It is a pleasure to thank Dr. D. Ballereau for permitting the use of the spectrum taken in Argentina. We also thank M. Ph. Moreau of the Haute Provence Observatory for the reproduction of the spectra. We thank the referee Prof. J.P. Swings for his careful reading of the paper.

References

Allen D.A., Swings J.P., 1976, A&A 47, 293
Andrillat Y, Houziaux L., 1967, J. Obs. 50, 107
Andrillat Y, Houziaux L., 1991, IAU Circ. 5164, 1
Bopp B.W., 1993, IBVS 3834, 1
Doazan V., 1960, Ann. Astrophys. 28, 1
Halbedel E., 1991, IBVS 3585, 1
Heck A., Egret D., Jaschek M., Jaschek C., 1984, A&AS 57, 213
Houziaux L., 1961, J. Obs. 43, 217
Hubert Delplace A.M., Hubert H., 1979, "Un atlas des étoiles Be" Observatoire de Paris-Meudon and Observatoire de Haute-Provence
Hutsemekers D., 1985, A&AS 60, 373
Hu Jingyao, Zhou Xu, 1990, Acta Astrophys. Sinica 10, 162
Jaschek M. , Hubert-Delplace A.M., Jaschek C., 1980, A&AS 42, 103
Jaschek C., Jaschek M., 1987, "The classification of stars". Cambridge University Press
Jaschek M., Jaschek C., Andrillat Y., Houziaux L., 1992, MNRAS 254, 413
Jaschek C., Jaschek M., 1993, A&AS 97, 807
Jaschek C., Andrillat Y, Jaschek M., 1996, A&AS 117, 281 (Paper I)
Johansson S., 1978, Phys. Scr. 18, 217
Kilkenny D., Whittet D.C.D., Davies J.K., Evans A., Bode M.F., Robson E.I., Banfield R.M., 1985, South African Astr. Obs. Circ. 9, 55
Lemaitre G., Kohler D., Lacroix D., Meunier J.P., Vin A., 1990, A&A 225, 545
Meinel A.B., Aveni A.F., Stockton M.W., 1969, "Catalog of emission lines in astrophysical objects", Tucson
Merrill P.W., Humason M., 1921, PASP 33, 112
Merrill P.W., 1931, ApJ 73, 348
Merrill P.W., 1952, ApJ 116, 501
Moore Ch., 1959, "A multiplet table of astrophysical interest" NBS Tech. Note 36
Morrison N.D., Beaver M., 1995, Bull. Amer. Astr. Soc. 27, 825
Nussbaumer M., Storey P.J., 1982, A&A 110, 295
Pogodin M.A., 1997, A&A 317, 185
Sitko M.L., Savage B.D., Meade M.R., 1981, ApJ 246, 161
Struve O., Swings P., 1940, PASP 52, 294
Swings P., Struve O., 1943, ApJ 98, 91
Thé P.S., de Winter D., Pérez M.R., 1994, A&AS 104, 315
Vaidya A., Schulte-Ladbeck R.E., Bjorkman K.S., 1994, Bull. Amer. Astr. Soc. 26, 933
Vaidya A., Schulte-Ladbeck R.E., 1995, Bull. Amer. Astr. Soc. 27, 825